CANCER BIOLOGY & THERAPY
2018, VOL. 19, NO. 3, 188–197
https://doi.org/10.1080/15384047.2017.1416274

Taylor & Francis
Taylor & Francis Group

RESEARCH PAPER

Temozolomide renders murine cancer cells susceptible to oncolytic adenovirus replication and oncolysis

Rodolfo Garza-Morales[a,d], Kavitha Yaddanapudi[b], Rigoberto Perez-Hernandez[a], Eric Riedinger[a], Kelly M. McMasters[a,b], Haval Shirwan[c], Esma Yolcu[c], Roberto Montes de Oca-Luna[d], and Jorge G. Gomez-Gutierrez [a,b]

[a]The Hiram C. Polk Jr, MD, Department of Surgery, University of Louisville School of Medicine, Louisville, KY, USA; [b]James Graham Brown Cancer Center, University of Louisville School of Medicine, Louisville, KY, USA; [c]Department of Microbiology and Immunology, Institute for Cellular Therapeutics, University of Louisville, Louisville, KY, USA; [d]Department of Histology, School of Medicine, Autonomous University of Nuevo León, Monterrey, N.L. México

ABSTRACT

The preclinical evaluation of oncolytic adenoviruses (OAds) has been limited to cancer xenograft mouse models because OAds replicate poorly in murine cancer cells. The alkylating agent temozolomide (TMZ) has been shown to enhance oncolytic virotherapy in human cancer cells; therefore, we investigated whether TMZ could increase OAd replication and oncolysis in murine cancer cells. To test our hypothesis, three murine cancer cells were infected with OAd (*E1b*-deleted) alone or in combination with TMZ. TMZ increased OAd-mediated oncolysis in all three murine cancer cells tested. This increased oncolysis was, at least in part, due to productive virus replication, apoptosis, and autophagy induction. Most importantly, murine lung non-cancerous cells were not affected by OAd+TMZ. Moreover, TMZ increased Ad transduction efficiency. However, TMZ did not increase coxsackievirus and adenovirus receptor; therefore, other mechanism could be implicated on the transduction efficiency. These results showed, for the first time, that TMZ could render murine tumor cells more susceptible to oncolytic virotherapy. The proposed combination of OAds with TMZ presents an attractive approach towards the evaluation of OAd potency and safety in syngeneic mouse models using these murine cancer cell-lines *in vivo*.

Abbreviations: Adhz60, OAd serotype 5 lacking the E1B gene; CAR, coxsackievirus and adenovirus receptor; CMV, cytomegalovirus.; CPE, cytopathic effect; GFP, green fluorescent protein; ivp, infectious viral particles; kDa, kilodaltons; KPCL, active oncogenic mutation in K-ras and loss-of-function in a p53 mouse model; LacZ, β-galactosidase; LC3, microtubule-associated protein 1A/1B-light chain 3; MOI, multiplicity of infection; OAds, oncolytic adenoviruses; TCID50, tissue culture infective dose 50; TMZ, temozolomide

ARTICLE HISTORY
Received 17 August 2017
Revised 7 December 2017
Accepted 7 December 2017

KEYWORDS
Adenovirus; cancer; murine; oncolytic; virotherapy

Introduction

One promising approach for the treatment of malignant tumors is the use oncolytic adenovirus (OAds). OAds have the ability to kill cancer cells via viral oncolysis, while leaving normal cells intact.[1] Even though OAds are known to replicate in and destroy human tumors, the preclinical characterization of OAds has, so far, been limited to immunodeficient xenograft tumor models.[2] Xenograft models are used because OAds for use in humans replicate poorly in murine tumor cells. The immunodeficient xenograft tumor model, however, does not allow for the evaluation of safety and efficacy profiles of OAds or the impact of a functional immune system on overall OAds potency. To more accurately model the study of OAds in the preclinical setting, an approach is needed that allows OAd replication and oncolysis in murine cancer cells lines.

There have been several recent advances toward the development of murine cancer cells that are permissive to OAd replication. Cheng et al.[3] reported that the ED-1 cell line derived from mouse lung adenocarcinoma overexpressing human cyclin E allowed OAd replication and oncolysis. In another study, Zhang et al.[4] found that the murine *K-ras*-induced lung adenocarcinoma cell line ADS-12 could be efficiently infected and OAd replication supported. Kang et al.[5] found that the expression of the coxsackievirus and adenovirus receptor (CAR), and E1b-55K genes enhanced adenovirus infectivity and replication in mouse melanoma cells.

We recently evaluated whether the alkylating agent temozolomide (TMZ) could enhance virotherapy potency in human lung cancer cells that are resistant (semi-permissive) to OAd-mediated oncolysis.[6] In the study abovementioned, we used an Ad serotype 5 containing a deletion of the entire Ad *E1B* gene that encodes both E1B19K and E1B55K proteins.[7] In this current study, we chose the same vector (Adhz60) to confirm that the findings in human cancer cells are reproducible in murine cancer cells. We found that TMZ-induced autophagy enhanced OAd replication and oncolysis in these semi-permissive lung cancer cell lines, and that the combination (OAd+TMZ) led to a synergistic cancer cell killing effect. Our data indicated that this enhanced anti-tumor activity was, at least in part, due to autophagy induction in these lung cancer cells. In the current

CONTACT Jorge G. Gomez-Gutierrez, PhD jgguti01@louisville.edu The Hiram C. Polk Jr, MD, Department of Surgery, University of Louisville School of Medicine, KCCTR Building, Room 452, 505 South Hancock, Louisville, KY, 40202, USA.

study, we evaluated whether treatment with TMZ could increase OAd replication and oncolysis in murine cancer cells. Our results suggest that the chemotherapeutic agent TMZ has the capability to increase OAd replication and oncolysis in all three murine cancer cells tested but not in non-cancerous cells. Furthermore, we believe that TMZ-treated murine cells will be a valuable tool to establish novel immunocompentent mouse models for the pre-clinical evaluation of the OAd-based therapies.

Results

Evaluation of OAd-mediated cytopathic effect and TMZ-induced cytotoxicity on murine cancer cells

Two murine cancer cells, KPCL and TC-1, cells were infected with an OAd serotype 5 lacking the E1B gene (Adhz60) at increasing concentrations of multiplicity of infection (MOI). At 72 hours post-infection, crystal violet staining revealed that cytopathic effect (CPE) increased in a virus dose-dependent manner in both cell lines (Fig. 1A). At an MOI concentration of 100, Adhz60 inhibited cell viability 40% in KPCL cells and 18% in TC-1 cells (Fig. 1B). KPCL and TC-1 cells also displayed OAd replication in a virus dose-dependent manner in murine cancer cells (Fig. 1C). These mouse cancer cell lines were then treated with increasing concentrations of TMZ. At 72 hours post-treatment, cell viability in the TMZ-treated cell lines decreased in a dose-dependent manner. Both KPCL and TC-1 displayed similar sensitivity to TMZ. The cell survival was approximately 60% at a concentration of 400 μM (Fig. 1D).

TMZ increases OAd-mediated CPE and productive virus replication in murine cancer cells but not in lung non-cancerous cells

Murine cancer and non-cancerous cells were infected with a replication-incompetent AdLacZ expressing β-galactosidase, which was used as a negative control for virus replication or Adhz60 and followed by either DMSO (vehicle control) or TMZ treatments. Crystal violet staining showed that TMZ increased the Adhz60-mediated CPE in both KPCL and TC-1 cells, whereas no CPE increase was observed in non-cancerous MM14.Lu cells (Fig. 2A). In KPCL cells treated with TMZ-alone or Adhz60-alone, the percentage of cell viabilities were 65% or 97%, respectively, whereas TMZ + Adhz60 combination treatment resulted in 20% of cell viability. A similar effect was observed in TC-1 cells; treatment with TMZ-alone or Adhz60-alone resulted in 55% or 80% of cell viability, respectively, whereas the combination treatment resulted in 10% of cell viability. The analysis of cell viabilities revealed that these differences in both cell lines were statistically significant (Fig. 2B, $^{*}P < 0.05$). In contrast, Adhz60+DMSO or Adhz60+TMZ treated-MM14.Lu cells displayed 88% and 81% of cell survival, respectively; this difference was not significant (Fig. 2B). As expected, AdLacZ did not induce CPE when used in combination with either DMSO or TMZ (Fig. 2B).

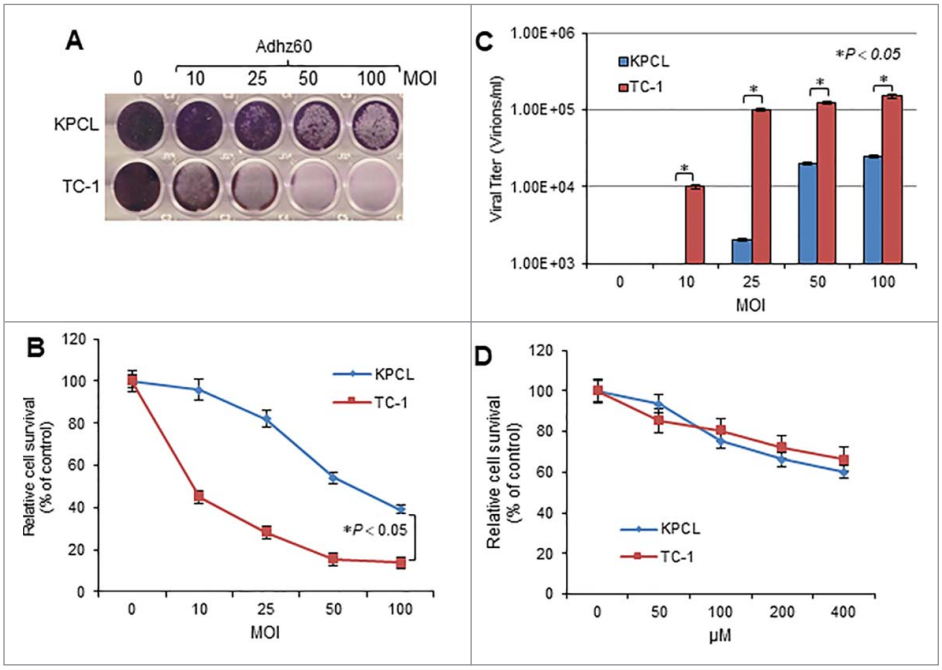

Figure 1. Evaluation of OAd-mediated cytopathic effect (CPE) and TMZ induced-cytotoxicity in murine cancer cells. (A) Murine lung cancer KPCL and TC-1 cell lines were infected with Adhz60 at a multiplicity of infection (MOI) concentration of 0, 10, 25, 50 and 100. At 72h post-infection, crystal violet staining was used to evaluate CPE. A representative staining is shown of three experiments performed. (B) OAd-mediated CPE was calculated by measuring the absorbance of solubilized dye at 590 nm. Each point represents the mean of three independent experiments ± standard deviation (SD; *bars*). (C) Supernatants were collected and used to determine adenovirus yield from each cell line. Results represent the mean of three independent experiments ± standard deviation (SD; *error bars*) ($^{*}P < 0.05$). (D) The cell lines above-mentioned were treated with TMZ at concentrations of 0, 50, 100, 200, and 400 μM. A MTT assay was used to determine cell survival at 72h post-treatment. Each point represents the mean of three independent experiments ± standard deviation (SD; *bars*).

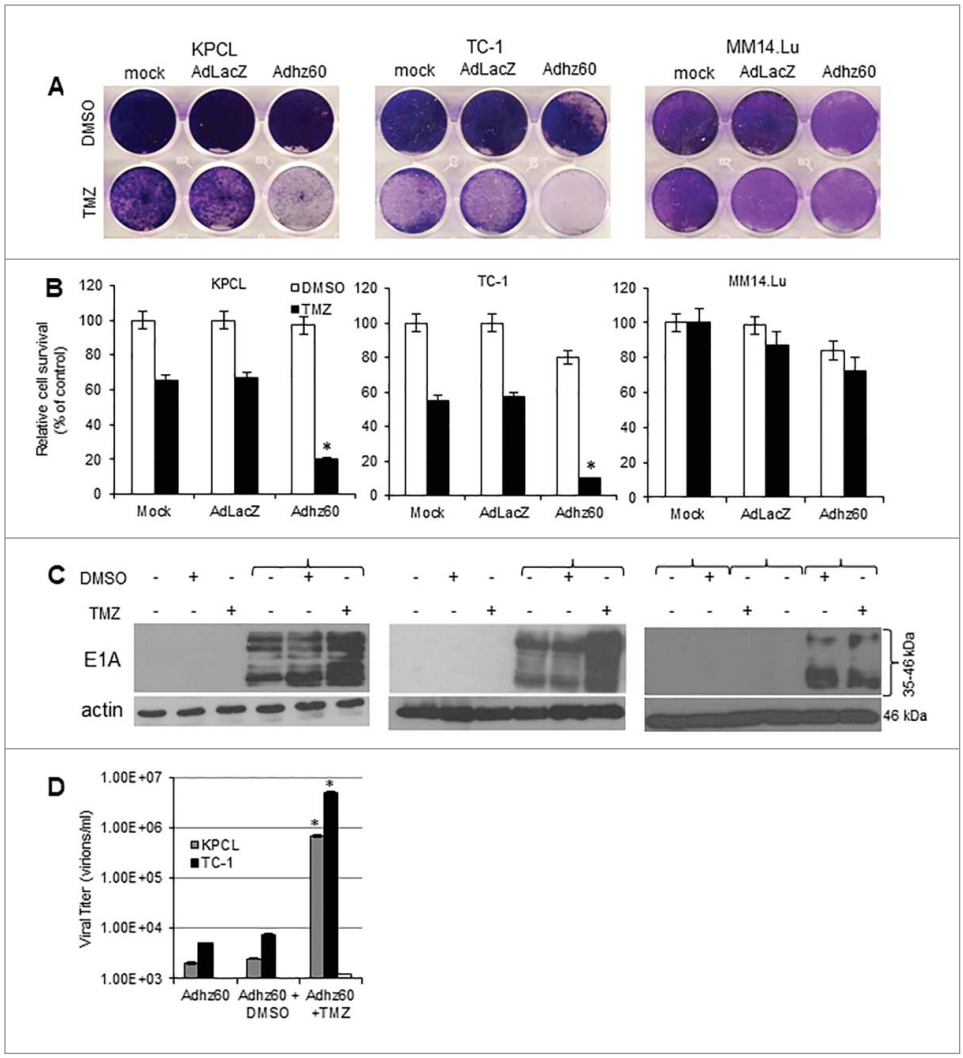

Figure 2. Effect of combined therapy of TMZ and OAd on virus replication in murine cancer and non-cancerous cells. (A) Murine cancer KPCL and TC-1 and non-cancerous MM14.Lu cells were treated with Adhz60 and TMZ at the following doses for Adhz60 and TMZ, respectively: (10 MOI, 400 μM). AdLacZ was used at 10 MOI for all cell lines. DMSO was added as a control at its respective volume for each cell line. At 72h post-infection, crystal violet staining was used to evaluate CPE. A representative staining is shown of three experiments performed. (B) OAd-mediated CPE was calculated by measuring the absorbance of solubilized dye at 590 nm. Results represent the mean of three repeated measurements ± standard deviation (SD; *error bars*) ($^*P < 0.05$ for all cell lines). (C) Expression of adenovirus E1A proteins were detected with an anti-adenovirus type 5 E1A monoclonal antibody. Actin was used as a loading control; a representative experiment is shown from three performed. (D) Supernatants from Fig. 2A were used to determine adenovirus yield from each cell line. Results represent the mean of three independent experiments ± standard deviation (SD; error bars) ($^*P < 0.05$).

To further assess the effect of TMZ upon Ad replication, Ad E1A and capsid hexon protein expressions and release of infective virus particles were evaluated. The adenovirus E1A region encodes two closely related gene products: 243 and 289 amino acid phosphoproteins. These proteins differ in their primary sequence only by 46 amino acids unique to the 289 amino acid protein.[8] An immunoblot assay revealed two main reactive species: the upper band corresponding to 46 kDa and a lower band corresponding to 35 kDa. It was found that TMZ increased E1A proteins expression in both KPCL and TC-1; whereas TMZ treatment did not increase E1A expressions in MM14.Lu cells (Fig. 2C). In a hexon immunostaining assay (supplemental online material 1A), cells infected with Adhz60 alone or in combination with DMSO showed approximately 13 and 11 hexon positive-cells, respectively. In KPLC or TC-1 cells, there were 16 and 18 hexon positive-cells, respectively. In contrast, KPCL or TC-1 cells treated with Adhz60 and TMZ displayed 22 and 47 hexon positive-cells, respectively. This difference was significant (supplemental online material 1B, $^*P < 0.05$). There was a two-fold increase in the number of hexon-positive cells in the presence of TMZ.

The supernatants from the combined treatment (Fig. 2A) were used to determine the release of infectious viral particles (ivp) by the TCID50 protocol in HEK293 cells. KPCL and TC-1 cells were shown to support production of ivp. In contrast, MM14.Lu cells were unable to produce ivp. TMZ increased Adhz60 virus production approximately 100-fold in KPCL and TC-1 cells in comparison with Adhz60-infected cells alone or in combination with drug vehicle control DMSO (Fig. 2D $^*P <$ 0.05). Overall, this suggests that TMZ increases Adhz60-mediated CPE in KPCL and TC-1 *via* increased Ad E1A expressions and productive virus replication. More importantly, the

combined therapy of OAd with TMZ did not induce CPE in MM14.Lu murine non-cancerous lung cells, making this approach safe for normal tissues.

TMZ increased Adhz60-mediated CPE was, at least in part, due to apoptosis induction

We investigated whether apoptosis could be associated with combined therapy-mediated CPE. Both TC-1 and KPCL cells were stained with Annexin V, and the percentage of total apoptosis was analyzed by FACScan flow cytometer (Fig. 3A). In TC-1 cells, TMZ-alone and Adhz60-alone induced 23.5% and 17.5% of late apoptosis, respectively, and the combined therapy induced 34% of total apoptosis (Fig. 3B; $^{*}P < 0.05$). TMZ-alone and Adhz60-alone-treated KPCL cells displayed 36.5% and 19.5% of total apoptosis, respectively. The combination (Adhz60+TMZ) resulted in 53% of total apoptosis (Fig. 3B; $^{*}P < 0.05$).

Apoptosis was further validated by detecting the endogenous expression of cleaved caspase-3. In KPCL cells, TMZ alone induced caspase-3 activation. Greater levels of cleaved caspase-3 were observed in Adhz60+TMZ treated-cells. A similar effect was observed in TC-1 cells (Fig. 3C).

Combined therapy of Adhz60 and TMZ induces greater autophagosomes formation and LC3-II accumulation than either agent alone

We previously demonstrated that TMZ induces autophagy in human lung cancer cells.[6] Therefore, the ability of TMZ to induce autophagy in murine cancer cells was evaluated. KPCL and TC-1 cell lines were transfected with pEGFP-LC3 followed by untreated or treated with either TMZ or Adhz60 alone or in combination. The formation of cytoplasmic punctate GFP fluorescence was then observed. The conversion of cytoplasm-diffuse GFP-LC3-I to membrane-associated GFP-LC3-II formed punctate patterns, indicating LC3-II incorporation into the autophagosomes. This formation of punctate was observed at 48 hours (Fig. 4A). TMZ-treated KPCL and TC-1 cells displayed significant accumulation of the fluorescent punctate pattern, from 6 to 29 and 3 to 24 GFP dots/cell, respectively (Fig. 4B). Adhz60-infected KPCL and TC-1 cells displayed a

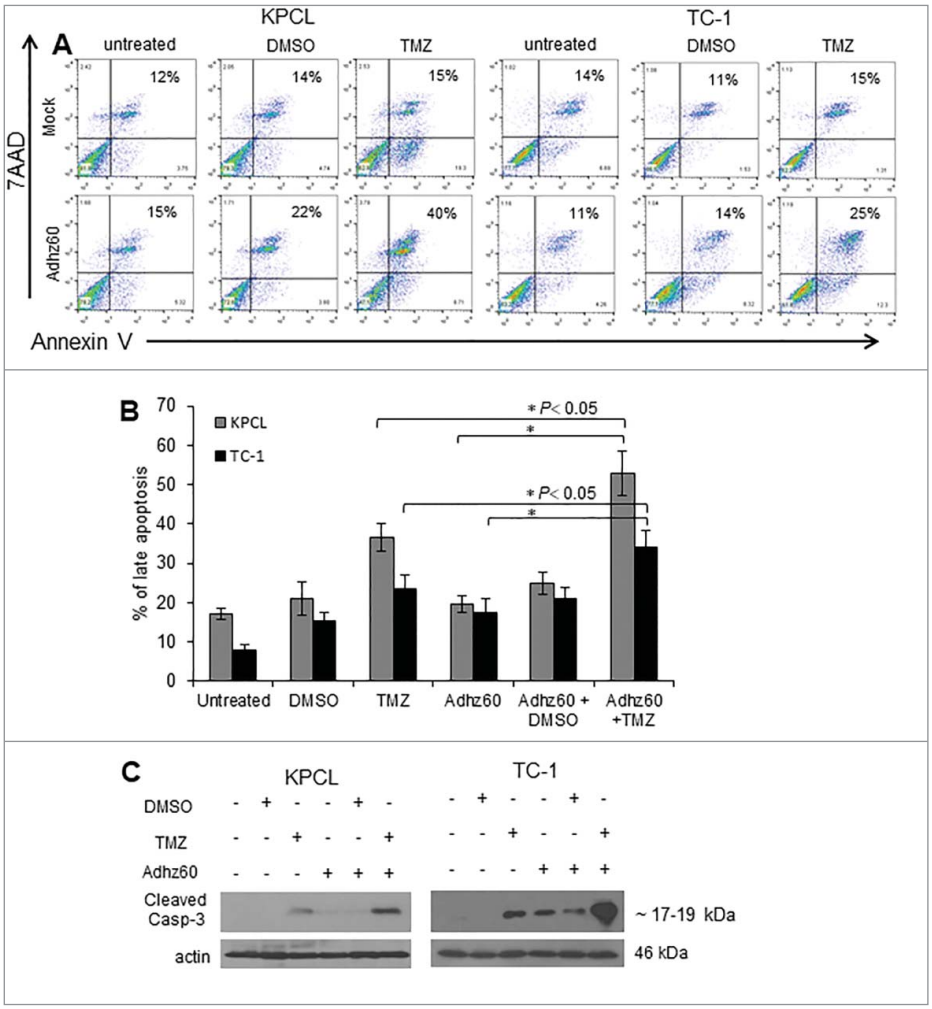

Figure 3. Evaluation of Adhz60 and TMZ combined therapy induced-apoptosis. Murine cancer cells were untreated or treated with DMSO, TMZ and Adhz60 alone or in combination as described in Fig. 2. (A) Seventy-two h post treatment, murine cancer cells were stained with annexin V-PE and 7-aminoactinomycin D (7-AAD). Positive cells for annexin V-PE and 7-AAD staining were analyzed by FACScan flow cytometer with FlowJo software. (B) Results represent the mean of three independent experiments ± standard deviation (SD; *error bars*) ($^{*}P < 0.05$). (C) Whole cell protein lysates were collected 72h after indicated treatment. Expression of cleaved caspase-3 was detected by western blot; actin was used as a loading control. A representative experiment is shown from three performed.

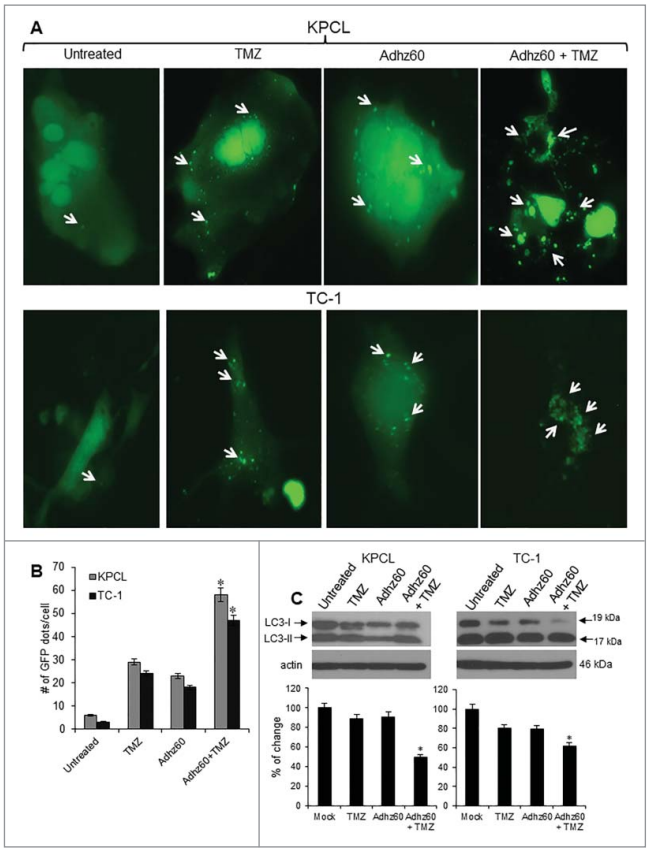

Figure 4. Evaluation of combined therapy ability to induce autophagy in mouse cancer cells. (A) Murine cancer cells were transfected with pEGFP-LC3 followed by untreated or treated with TMZ at 400 μM or Adhz60 at an MOI concentration of 10 alone or in combination. Integration of GFP-LC3 into the autophagosome is depicted by punctate structures and was analyzed by fluorescence microscopy at 48h post-treatment. Images were taken at 40× magnification with the EVOS FL Imaging System (Advanced Microscopy Group) under 357/44 (nm) and 447/60 (nm) excitation and emission visualization. Comparison of number of GFP dots per cell in untreated cells or treated with TMZ, Adhz60 or combination of both. A representative experiment showing punctate (arrows) is shown from three performed. (B) Comparison of number of GFP dots per cell in untreated or treated cells with TMZ, Adhz60 or combination of both. A representative experiment is shown from three performed. (C)Whole cell protein lysates were collected 72h after indicated treatment. Western blot and bar graphs of LC3-I and II expressions. Bars represent mean ± SEM expressed as percentage of change from 3 separate experiments, ($^{*}P < 0.05$) decrease in the level of LC3-I expression. Actin was used as a loading control.

similar effect, from 6 to 23 and 3 to 18 GFP dots/cell, respectively (Fig. 4B). Greater fluorescent punctate pattern accumulation was observed in combined therapy-treated KPCL and TC-1 cells, from 58 and 47 GFP dots/cell, respectively (Fig. 4B).

The conversion of LC3-I to LC3-II is considered an autophagy marker and used to detect autophagy induction.[9] We evaluated autophagy induction in murine cancer cells after treatment with TMZ and Adhz60 either independently or in combination. An immunoblot analysis revealed two reactive LC3 species: the upper band corresponding to LC3-I (19 kDa) and a lower band corresponding to LC3-II (17 kDa). KPCL and TC-1 cells infected with Adhz60 displayed a clear decrease in LC3-I expression levels (Fig. 4C). A marked accumulation of LC3-II was observed in Adhz60 + TMZ-treated cells as compared to untreated TMZ or Adhz60-treated cells (Fig. 4C, $^{*}P < 0.05$). These results suggest that the combination of Adhz60 and TMZ induced a significant decrease in LC3-I and LC3-II accumulation than that observed when cells were treated with either agent alone. The increased LC3-II accumulation in Adhz60 + TMZ-treated cells may be, at least in part, due to increased virus replication (Fig. 2).

TMZ increases OAd-mediated CPE in mouse triple-negative breast cancer cells

To determine whether TMZ could enhance adenovirus-mediated oncolysis in mouse triple-negative breast cancer (TNBC) cells, mouse TNBC 4T1 cells were treated with the combined therapy or the respective controls. CPE was observed only in instances where the combination Adhz60 + TMZ was used; by contrast, in Adhz60 or TMZ-alone treatment groups (Fig. 5A), no significant CPE was observed. The analysis of murine breast cancer cell viability revealed that these differences were statistically significant (Fig. 5B, $^{*}P < 0.05$). Virus production increased in Adhz60 + TMZ-treated cells relative to those observed in Adhz60-alone or Adhz60+DMSO-treated cells (Fig. 5C, $^{**}P < 0.01$).

To determine whether the combination of Adhz60 with TMZ could induce greater autophagy induction than treatment with either of the agents independently, 4T1 cells were treated independently with TMZ or Adhz60 at indicated doses or in combination. At 72 hours post-treatment, autophagy induction was evaluated by LC3-I to LC3-II conversion (Fig. 5D). Untreated cells displayed no LC3-II accumulation; in contrast, TMZ treatment induced LC3-II accumulation, while Adhz60-alone slightly induced the conversion of LC3-I to LC3-II. LC3-II induction was greater in cells treated with Adhz60 + TMZ (Fig. 5D, $^{*}P < 0.05$).

In addition, the percentage of apoptotic cells was determined by annexin V staining and flow cytometry analysis (Fig. 5E). Our results indicate that the percentage of apoptotic cells was more increased in the viral-chemotherapy combination than any single treatment (Fig. 5E). When used independently, TMZ and Adhz60 induced 17%, and 18% of total apoptosis, respectively (Fig. 5F). A significantly higher apoptosis (66%) was induced in cells when treated with Adhz60+TMZ combination. The difference between single treatment and combined therapy was significant (Fig. 5F, $^{*}P < 0.05$).

Apoptosis induction was further validated by detection of endogenous cleaved caspase-3. TMZ-alone induced caspase-3 activation, whereas Adhz60 or Adhz60 + DMSO-treated cells slightly induced caspase-3 activation; however, the combination of Adhz60 and TMZ induced greater caspase-3 activation (Fig. 5G). These data suggest that TMZ treatment appears to increase the susceptibility of mouse breast cancer cells to OAd replication and oncolysis. These findings also suggest that the viral-chemotherapy-mediated cytotoxicity induces apoptosis as a mechanism of cell death in addition to oncolysis.

TMZ increases Ad transduction efficiency in murine cancer cells but not coxsackievirus and adenovirus receptor

To determine whether TMZ may affect Ad transduction efficiency positively, murine cancer cells were infected with replication-defective Ad expressing green fluorescent protein

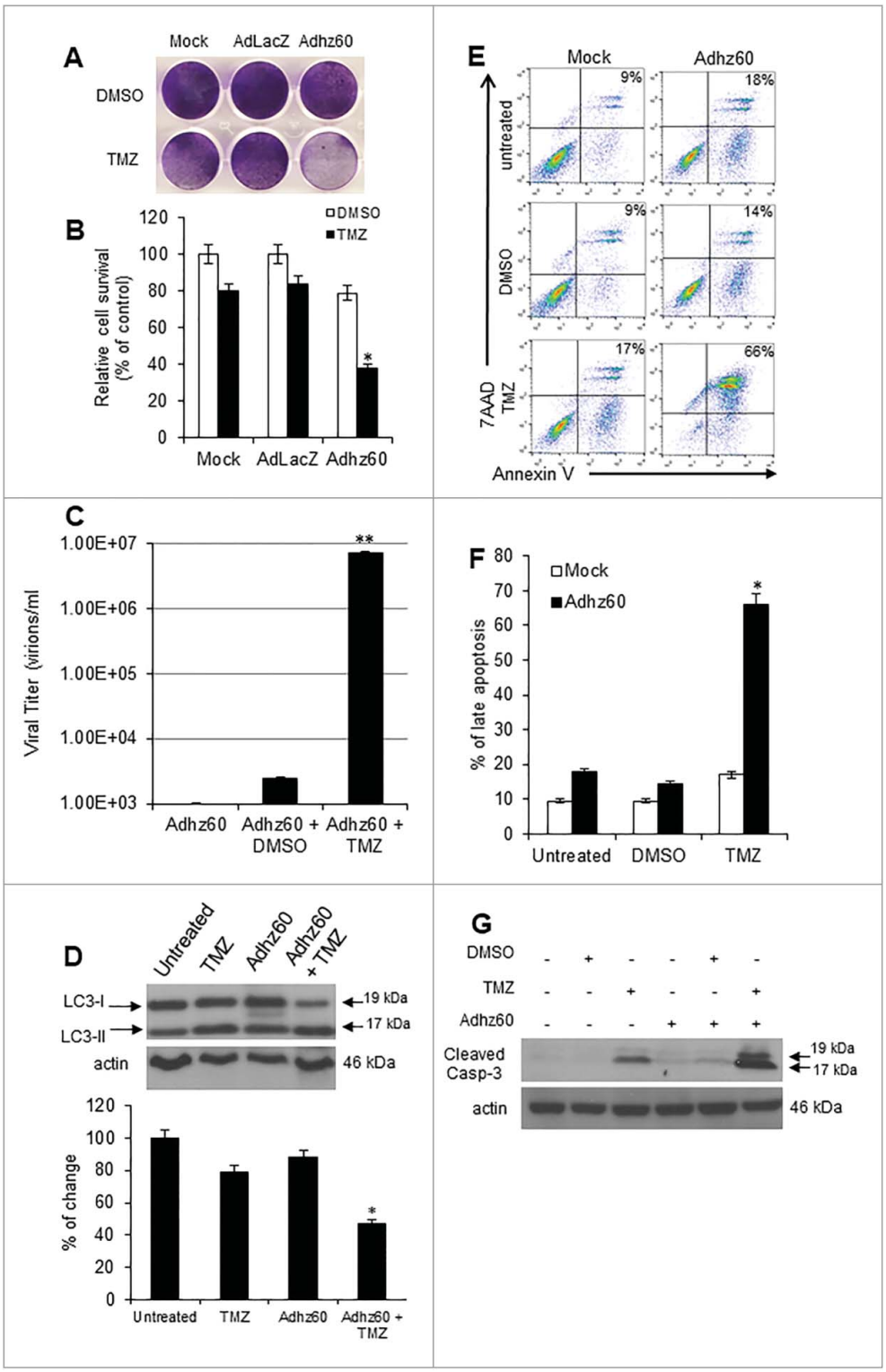

Figure 5. Effect of TMZ on OAd-mediated CPE in murine triple negative breast cancer cells. 4T1 Murine breast cancer cells were no treated (Mock) or treated with Adhz60 and TMZ at the following doses for Adhz60 and TMZ, respectively: (10 MOI and 400 μM). AdLacZ was used at 10 MOI. DMSO was added as a control. (A) Cytopathic effect was evaluated by crystal violet staining at 72 hours following treatment and reported as percentage of control (mock). (B) Cell viability was calculated by measuring the absorbance of solubilized dye at 590 nm. Results represent the mean of three repeated measurements $\pm$ standard deviation (SD; *error bars*) ($^{*}P < 0.05$). (C) Seventy-two hours post-treatment, supernatants were collected and used to determine virus adenovirus yield from each cell line. Results represent the mean of three independent experiments $\pm$ standard deviation (SD; *error bars*) ($^{**}P < 0.01$). (D) Whole cell protein lysates were collected 72h after indicated treatment. Western blot and bar graphs of LC3-I and II expressions. Bars represent mean $\pm$ SEM expressed as percentage of change from 3 separate experiments, ($^{*}P < 0.05$) decrease in the level of LC3-I expression. Actin was used as a loading control. (E) Cells were stained with annexin V-PE and 7-aminoactinomycin D (7-AAD). Positive cells for annexin V-PE and 7-AAD staining were analyzed by FACScan flow cytometer. (F) Results represent the mean of three independent experiments $\pm$ standard deviation (SD; *error bars*) ($^{*}P < 0.05$). (G) Whole cell protein lysates were collected 72h after indicated treatment. Expression of cleaved caspase-3 was detected by western blot; actin was used as a loading control. A representative experiment is shown from three performed.

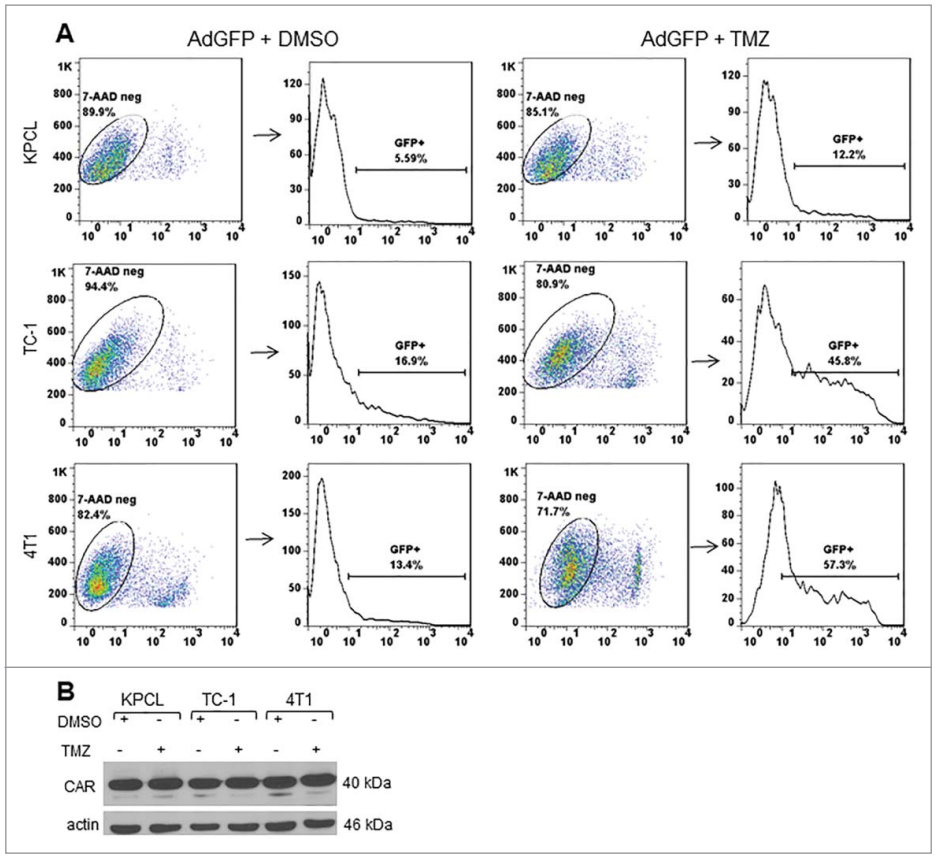

Figure 6. Effect of TMZ on Ad transduction efficiency and expression of coxsackie adenovirus receptor. Murine cancer cells were infected with AdGFP at an MOI of 10 followed by DMSO or TMZ at 400 μM. (A) Forty-eight h post treatment, cells were collected and GFP expression was analyzed by FACScan flow cytometer (Becton Dickinson, Franklin Lakes, NJ) and with FlowJo software (Tree Star Inc., Ashland, OR). A representative experiment is shown from three performed. (B) Expression of coxsackie adenovirus receptor was detected with an antibody that can recognize both human and mouse CAR. Actin was used as a loading control, a representative experiment is shown from three performed.

(AdGFP) in the presence of either DMSO or TMZ. At 48 hours post-treatment, the percentage of GFP-positive cells was determined by FACScan flow cytometer. 7AAD was used as a cell viability marker. Only 7AAD-negative and GFP-positive cells were counted. In KPCL cells with DMSO, 5% of cells were positive for GFP. In the presence of TMZ, there was an increase to 12% of GFP-positive cells (Fig. 6A). TC-1 and 4T1 cells displayed 16% and 13% of GFP-positive cells with DMSO, respectively. GFP expression increased to 45% and 57%, respectively, in the presence of TMZ (Fig. 6A). In addition, expression of coxsackievirus and adenovirus receptor (CAR) was evaluated. No difference in CAR expression was observed in either DMSO or TMZ-treated cells (Fig. 6B). This suggests that there are other mechanisms involved in the increased Ad transduction capability of murine cancer cells. This result suggests that TMZ affects positively the Ad transduction efficiency at least in murine cancer cells tested.

Discussion

Oncolytic adenoviruses have been shown to replicate in and destroy human tumors, however, the OAd preclinical characterization has been restricted to immunodeficient xenograft tumor models.[2] Immunodeficient xenograft models have been used because human OAds replicate poorly in murine tumor cells. The immunodeficient xenograft tumor model, however, does not effectively evaluate the efficacy, safety profiles, how the immune system impacts OAds effectiveness, or whether it contributes to vector potency. Therefore, identifying mouse cancer cells that are permissive for OAd replication is needed for the development of immunocompetent murine models to evaluate the pre-clinical effects of virotherapy in a manner that better approximates the treatment of cancer patients clinically. Some progress has been made in developing oncolytic viruses that can replicate in mouse cancer cells.[10-12] Previously, it was reported that the ED-1 cell line derived from mouse lung adenocarcinomas overexpressing human cyclin E allowed OAd replication and oncolysis.[3] In other study, it was found that the murine K-ras-induced lung adenocarcinoma cell line ADS-12 supported adenoviral infection and OAd replication.[4] It was also reported that the expression of the coxsackievirus, adenovirus receptor (CAR), and E1b-55K genes enhanced adenovirus infectivity and replication in mouse melanoma cells.[5]

We recently found that semi-permissive lung cancer cells are efficiently destroyed by oncolytic adenovirus in combination with TMZ.[6] This enhanced killing effect was due to enhanced apoptosis, virus replication, and autophagy induction. In a lung cancer xenograft model, the combination of TMZ and Adhz60 therapy displayed superior tumor growth suppression than either each treatment alone. In this study, we evaluated the capability of TMZ to increase OAd replication and oncolysis in murine cancer cells as address the need for an improved

approach to evaluate OAds in three syngeneic mouse cancer models.

Human OAds replicate poorly in murine tumor cells,[2] but it is possible that *E1b*-deleted OAds replicate more efficiently in HPV-16-*E6/E7*-positive murine cancer cells (TC-1) because HPV E6 or E7 expressing tumor cells can support the DNA replication of *E1a*- and *E1b*-deleted adenoviruses.[13,14] The HPV-16 E7 open reading frame specifically is known to encode transcriptional transactivation and cellular transformation functions, which are analogous to those of adenovirus E1A protein.[15] Therefore, the presence of HPV-16-*E6*/E7 in TC-1 cells may transcomplement Adhz60 (lacking the Ad *E1b* gene) and explain why Adhz60 has a greater replication and oncolysis in TC-1 than in KPCL cells.

Both TC-1 and KPCL cells contains oncogenes (i.e., E6/E7, c-Ha-ras and K-ras respectively) that may contribute to their ability to support OAd-mediated oncolytic cell death. One piece of evidence is that the murine K-ras-induced lung adenocarcinoma cell line ADS-12 supports adenoviral infection and generates infectious viral progeny.[4] This suggests that cancer cells expressing significant levels of at least c-Ha-ras and/or K-ras oncogenes may be excellent candidates for OAd therapy.

TMZ likely rendered 4T1 cells more susceptible to OAd replication and oncolysis, thus increasing OAd efficacy in combination with TMZ. These 4T1 cells are the current standard animal model for highly aggressive, metastatic human BC stage IV or triple-negative BC.[16] Therefore, these findings open up the possibility to evaluate the combination therapy of OAd with TMZ in an immunocompetent mouse model of TNBC and thus to assess the safety and efficacy profiles of these OAds and the impact of an active immune system upon overall OAds efficacy.

Autophagy is an essential mechanism for cells to degrade unnecessary or dysfunctional cellular components. The breakdown of these components can ensure cell survival during starvation and stress by maintaining cellular energy homeostasis. Autophagy has a dual role, acting as a survival mechanism and as a caspase-independent form of programmed cell death.[17,18] Although we do not know the precise mechanism by which TMZ increased Ad transduction efficiency in murine cancer cells, it is possible that TMZ mediated-autophagic stress may weaken cell membranes facilitating Ad entry into the cell. Mitochondrial depolarization and permeability transition pore (MPTP) opening was observed as a prelude to TMZ-induced autophagy. These were followed by the loss of mitochondrial mass.[19]

In summary, we report, for the first time, that TMZ, an alkylating chemotherapy drug, is able to increase OAd replication and oncolysis in murine lung and breast cancer cells. These findings can lead to developing valuable tools that can be used to test the efficacy, safety, and impact of OAds in a preclinical immunocompetent mouse models that are more comparable to cancer patients than xenograft mouse models.

Materials and methods

Cell lines and culture conditions

Murine lung or bronchus non-cancerous cells MM14.Lu (Cat # CRL-6382), murine triple-negative estrogen receptor breast cancer (TNBC) 4T1 (Cat # CRL-2539), lung cancer TC-1 (Cat # CRL-2785) cells derived from primary epithelial cells of C57BL/6 mice co-transformed with HPV-16 E6/E7, and the c-Ha-ras and human embryonic kidney cell line HEK-293 (Cat # CRL-1573) were all purchased from the American Type Culture Collection (ATCC). The mouse non-small cell lung carcinoma (NSCLC) cell line KPCL containing an active oncogenic mutation in K-ras and loss-of-function in a p53 was derived from K-ras$^{LSL\text{-}G12D/+}$;p53$^{fl/fl}$(B6) transgenic C57BL/6 mice, was kindly provided by Dr. Zippelius, Department of Biomedicine, University Hospital Basel, Switzerland.[20] MM14.Lu, KPCL, and HEK-293 cells were grown in DMEM (Cat # 10-013-CV); TC-1 and 4T1 cells were cultured in RPMI-1640 (Cat # 10-040-CV). All media were supplemented as described previously.[21] All cell culture reagents were obtained from Corning Cellgro.

Adenoviral vectors and drugs

Two replication-deficient adenoviral vectors expressing either β-galactosidase (AdLacZ) or green fluorescent protein (AdGFP) under regulation of the CMV promoter were used as a negative control for virus replication or for transduction efficiency assay as described previously.[21,22] The conditionally replicating adenovirus (Adhz60, *E1b*-deleted) was used as previously reported by us.[7] Temozolomide (TMZ, Cat # T2577) stock solution of 100 mM was prepared in dimethyl sulfoxide (DMSO, Cat # D8418) and stored at -20°C. TMZ and DMSO were purchased from (Sigma-Aldrich). The volume of TMZ or DMSO added to the cell cultures was less than 1%.

Single and combined therapies

A total of 2.5×10^4 cells were plated in 24-well plates and treated after 24 hours as indicated. Viral infection was performed at the indicated MOI concentrations, whereas TMZ or 4-hydroxytamoxifen (TAM) treatments were performed at the micromolar (μM) concentrations as indicated. Adhz60-mediated CPE was evaluated at 72 hour post-infection by crystal violet staining. Suspended cells were removed by aspiration. The remaining adherent cells were then fixed with 3.7% formaldehyde for 3 min at room temperature. The excess formaldehyde was washed with phosphate buffered saline. The cells were then stained using 1% crystal violet at room temperature for 3 min. Excess crystal violet was washed away with PBS. Plates were scanned using an HP Scanjet 4070 scanner (HP, Palo Alto, CA, USA). The remaining crystal violet was then solubilized with a 2% sodium dodecyl sulfate (SDS) solution, and the sample absorbances were measured at 590 nm using a Synergy HT Multi-Mode Microplate Reader (Bio-Tek, Winooski, VT, USA). The absorbance (OD) values of each treatment were then normalized to mock-treated cells converting each sample OD into the percent of cell viability according to the formula previously by our group.[23]

$$Cellviability\,\% = (ODoftreatedcells\ /\ ODofmock - treatedcells) \times 100\%$$

Temozolomide-mediated inhibition of cell viability was assessed 72 hours after treatment by measuring the conversion

the tetrazolium salt 3-(4,5-dimethylthiazol-2-yl)-2,5-diphenyltetrazolium (MTT) to formazan according to the manufacturer's instructions (Sigma Aldrich, Cat # M2128) and as described by our group.[21] The supernatant from each plate was collected for measurement of absorbance at a wavelength of 570 nm. The results are expressed as the percentage of live cells. For therapeutic negative control treatment groups, we used cell line-specific media alone without virus treatment (mock) or drug vehicle (DMSO) instead of TMZ. For combined therapies, cells were treated with Adhz60 and TMZ at the indicated concentrations respectively. At 72 hours post-treatment, cell viability was evaluated by crystal violet assay as described above.

Annexin V staining

Cells were treated with the respective single or combined agents 72 hours post-treatment. The nonadherent cells were harvested, and adherent cells were trypsinized for 1 minute and then stopped with PBS/10% FCS. Nonadherent cells and adherent cells were pulled and stained with annexin V-PE and 7-AAD according with the manufacturer's instructions (BD Pharmingen, Cat # 559763) and as reported previously.[24] Cells were analyzed by FACScan flow cytometer (Becton Dickinson) and with FlowJo software (Tree Star Inc.).

Adenovirus titer assay

For production of infectious virus particles measurement, cells were infected with Ahz60-alone or treated as described in the combined therapies section. At 72 hours post-treatment, supernatants were collected (1 ml) and centrifuged for 10 min at 14,000 rpm. Supernatants were transferred to a new 1.5 ml tube to eliminate the cell debris and/or cells in suspension that may have contained Ads. Supernatants were diluted serially by using median tissue culture infective dose or the amount of a pathogenic agent that will produce pathological change in 50% of cell cultures inoculated (TCID50) or by using the end-point dilution method with HEK-293 cells seeded on 96-well plates as described previously.[25]

Western blot analysis

Cells were harvested and lysed in RIPA buffer as described previously.[26] Cell lysates were centrifuged, and protein concentration was determined by PIERCE BCA Protein Assay kit (Thermo Scientific, Cat # 23225). Equal amounts of cellular protein were electrophoresed in 10% or 12% SDS-polyacrylamide gels and transferred to Hybond-PVDF membranes (GE, Healthcare, Life Sciences, Cat # 10600023). The membranes were first incubated with the following primary antibodies: mouse anti-adenovirus type 5 E1A (BD Pharmingen, Cat # 554155), rabbit anti-LC3 polyclonal antibody (Sigma-Aldrich, Cat # L7543), rabbit anti-cleaved caspase-3 (Cell signaling, Cat # 9664), rabbit anti-coxsackie adenovirus receptor (abcam, Cat # 02139-1517), and rabbit-antihuman-actin (Sigma-Aldrich, Cat # A2066). Next, the membranes were incubated with anti-mouse immunoglobulin (Ig) or anti-rabbit Ig, peroxidase-linked, species-specific whole antibody (Thermo Scientific, Cat # 31430 and 31460 respectively). ECL reagents were used to detect the signals according to the manufacturer's instructions (GE Healthcare, Cat # RPN3244). All films were scanned with an optical scanner (Epson Expression 1680) and quantified by measuring the density of each band using UNSCAN-IT software (Silk Scientific, Inc; Orem, UT). To correct for possible unequal loading, each band's density was normalized to its α-actin density. To allow for multiple comparisons between films, each sample was compared to its respective mock (not infected) or not treated that was run on the same gel. Results are expressed in percentage of change that was calculated by dividing the averages of each protein band.[22]

GFP-LC3 puncta

Plasmid vector containing green fluorescent protein (GFP) linked to microtubule-associated protein 1 light chain 3 (LC3)[9] was used to detect autophagosome formation in lung cancer cell lines. At 24 hours post-transfection, cells were untreated or treated with TMZ at 400 μM or Adhz60 at an MOI concentration of 10 alone or in combination. At 48 hours post-treatment, cells were examined under a fluorescence microscope. Cells were classified as having a predominantly diffuse GFP stain or having numerous punctate structures representing autophagosomes. Images were taken at 40× magnification with the EVOS FL Imaging System (Advanced Microscopy Group) under 357/44 (nm) and 447/60 (nm) excitation and emission visualization. The percentage of cells with GFP puncta were calculated as the proportion of cells with GFP puncta divided by the total number of GFP expressing cells.

Hexon immunostaining

TC-1 or KPCL cells (5×10^4) were seeded on a 24-well plate overnight. These cells were infected the next day with Adhz60 at an MOI of 10 followed by either DMSO or TMZ (400 μM). At 48 hours post-infection, hexon immunostaining was performed according with the manufacturer's instructions (Takara Clontech, Cat # 632250). The number of hexon-positive cells was calculated as brown-positive cells per total cell number in the field imaged at 20x objective magnification in three different fields.

Adenovirus transduction efficiency assay

Murine cancer cells were plated in a 6-well plate at a density of 1×10^5 cells per well. Cells were infected the next day with AdGFP at an MOI concentration of 10 followed by DMSO vehicle drug control or TMZ at 400 μM. At 48 hours post-treatment, cells were collected, and GFP expression was analyzed by FACScan flow cytometer (Becton Dickinson, Franklin Lakes, NJ) and with FlowJo software (Tree Star Inc., Ashland, OR).

Statistical analysis

The results of the *in vitro* assays were analyzed by unpaired Student's *t* test using a one-way ordinary parametric analysis of variance. A significance level of $P < 0.05$ was considered statistically significant.

Disclosure of potential conflicts of interest

No potential conflicts of interest were disclosed.

Acknowledgments

This work was supported by National Institutes of Health NCI award R25CA134283 (ER and RP-H.) and in part by NIH/NCI award R21CA210202 (JGGG). We thank Margaret Abby for editing.

Funding

HHS | NIH | National Cancer Institute (NCI) (R25-CA-134283).
HHS | NIH | National Cancer Institute (NCI) (R21-CA-210202).

ORCID

Jorge G. Gomez-Gutierrez http://orcid.org/0000-0003-3610-260X

References

1. Nettelbeck DM. Cellular genetic tools to control oncolytic adenoviruses for virotherapy of cancer. J Mol Med (Berl). 2008;86:363–77. doi:10.1007/s00109-007-0291-1.
2. Robinson M, Li B, Ge Y, Ko D, Yendluri S, Harding T, VanRoey M, Spindler KR, Jooss K. Novel immunocompetent murine tumor model for evaluation of conditionally replication-competent (oncolytic) murine adenoviral vectors. J Virol. 2009;83:3450–62. doi:10.1128/JVI.02561-08.
3. Cheng PH, Rao XM, Wechman SL, Li XF, McMasters KM, Zhou HS. Oncolytic adenovirus targeting cyclin E overexpression repressed tumor growth in syngeneic immunocompetent mice. BMC Cancer. 2015;15:716. doi:10.1186/s12885-015-1731-x.
4. Zhang L, Hedjran F, Larson C, Perez GL, Reid T. A novel immunocompetent murine model for replicating oncolytic adenoviral therapy. Cancer Gene Ther. 2015;22:17–22. doi:10.1038/cgt.2014.64.
5. Kang S, Kim JH, Kim SY, Kang D, Je S, Song JJ. Establishment of a mouse melanoma model system for the efficient infection and replication of human adenovirus type 5-based oncolytic virus. Biochem Biophys Res Commun. 2014;453:480–5. doi:10.1016/j.bbrc.2014.09.107.
6. Gomez-Gutierrez JG, Nitz J, Sharma R, Wechman SL, Riedinger E, Martinez-Jaramillo E, Sam Zhou H, McMasters KM. Combined therapy of oncolytic adenovirus and temozolomide enhances lung cancer virotherapy in vitro and in vivo. Virology. 2016;487:249–59. doi:10.1016/j.virol.2015.10.019.
7. Rao XM, Tseng MT, Zheng X, Dong Y, Jamshidi-Parsian A, Thompson TC, Brenner MK, McMasters KM, Zhou HS. E1A-induced apoptosis does not prevent replication of adenoviruses with deletion of E1b in majority of infected cancer cells. Cancer Gene Therapy. 2004;11:585–93. doi:10.1038/sj.cgt.7700739.
8. Lillie JW, Green M, Green MR. An adenovirus E1a protein region required for transformation and transcriptional repression. Cell. 1986;46:1043–51. doi:10.1016/0092-8674(86)90704-X.
9. Kabeya Y, Mizushima N, Ueno T, Yamamoto A, Kirisako T, Noda T, Kominami E, Ohsumi Y, Yoshimori T. LC3, a mammalian homologue of yeast Apg8p, is localized in autophagosome membranes after processing. EMBO J. 2000;19:5720–8. doi:10.1093/emboj/19.21.5720.
10. Eggerding FA, Pierce WC. Molecular biology of adenovirus type 2 semipermissive infections. I. Viral growth and expression of viral replicative functions during restricted adenovirus infection. Virology. 1986;148:97–113. doi:10.1016/0042-6822(86)90406-X.
11. Ginsberg HS, Moldawer LL, Sehgal PB, Redington M, Kilian PL, `Chanock RM, Prince GA. A mouse model for investigating the molecular pathogenesis of adenovirus pneumonia. Proc Natl Acad Sci U S A. 1991;88:1651–5. doi:10.1073/pnas.88.5.1651.
12. Silverstein G, Strohl WA. Restricted replication of adenovirus type 2 in mouse Balb/3T3 cells. Arch Virol. 1986;87:241–64. doi:10.1007/BF01315303.
13. Steinwaerder DS, Carlson CA, Lieber A. DNA replication of first-generation adenovirus vectors in tumor cells. Hum Gene Therapy. 2000;11:1933–48. doi:10.1089/10430340050129549.
14. Steinwaerder DS, Carlson CA, Lieber A. Human papilloma virus E6 and E7 proteins support DNA replication of adenoviruses deleted for the E1A and E1B genes. Mol Therapy: J Am Soc Gene Therapy. 2001;4:211–6. doi:10.1006/mthe.2001.0447.
15. Phelps WC, Yee CL, Munger K, Howley PM. The human papillomavirus type 16 E7 gene encodes transactivation and transformation functions similar to those of adenovirus E1A. Cell. 1988;53:539–47. doi:10.1016/0092-8674(88)90570-3.
16. Aslakson CJ, Miller FR. Selective events in the metastatic process defined by analysis of the sequential dissemination of subpopulations of a mouse mammary tumor. Cancer Res. 1992;52:1399–405.
17. Gozuacik D, Kimchi A. Autophagy and cell death. Curr Top Dev Biol. 2007;78:217–45. doi:10.1016/S0070-2153(06)78006-1.
18. Newman RA, Kondo Y, Yokoyama T, Dixon S, Cartwright C, Chan D, Johansen M, Yang P. Autophagic cell death of human pancreatic tumor cells mediated by oleandrin, a lipid-soluble cardiac glycoside. Integr Cancer Ther. 2007;6:354–64. doi:10.1177/1534735407309623.
19. Lin CJ, Lee CC, Shih YL, Lin CH, Wang SH, Chen TH, Shih CM. Inhibition of mitochondria- and endoplasmic reticulum stress-mediated autophagy augments temozolomide-induced apoptosis in glioma cells. PloS One. 2012;7:e38706. doi:10.1371/journal.pone.0038706.
20. Wieckowski S, Hemmerle T, Prince SS, Schlienger BD, Hillinger S, Neri D, Zippelius A. Therapeutic efficacy of the F8-IL2 immunocytokine in a metastatic mouse model of lung adenocarcinoma. Lung Cancer. 2015;88:9–15. doi:10.1016/j.lungcan.2015.01.019.
21. Egger ME, McNally LR, Nitz J, McMasters KM, Gomez-Gutierrez JG. Adenovirus-mediated FKHRL1/TM sensitizes melanoma cells to apoptosis induced by temozolomide. Human gene therapy Clin Dev. 2014;25:186–95. doi:10.1089/humc.2014.022.
22. Gomez-Gutierrez JG, Egger ME, Hao H, Zhou HS, McMasters KM. Adenovirus-mediated expression of mutated forkhead human transcription like-1 suppresses tumor growth in a mouse melanoma xenograft model. Cancer Biol Ther. 2012;13:1195–204. doi:10.4161/cbt.21349.
23. Wechman SL, Rao XM, Cheng PH, Gomez-Gutierrez JG, McMasters KM, Zhou HS. Development of an oncolytic Adenovirus with enhanced spread ability through repeated UV irradiation and cancer selection. Viruses. 2016;8:E167. doi:10.3390/v8060167.
24. Gomez-Gutierrez JG, Garcia-Garcia A, Hao H, Rao XM, Montes de Oca-Luna R, Zhou HS, McMasters KM. Adenovirus-mediated expression of truncated E2F-1 suppresses tumor growth in vitro and in vivo. Cancer. 2010;116:4420–32. doi:10.1002/cncr.25322.
25. Rodriguez-Rocha H, Gomez-Gutierrez JG, Garcia-Garcia A, Rao XM, Chen L, McMasters KM, Zhou HS. Adenoviruses induce autophagy to promote virus replication and oncolysis. Virology. 2011;416:9–15. doi:10.1016/j.virol.2011.04.017.
26. Gomez-Gutierrez JG, Souza V, Hao HY, Montes de Oca-Luna R, Dong YB, Zhou HS, McMasters KM. Adenovirus-mediated gene transfer of FKHRL1 triple mutant efficiently induces apoptosis in melanoma cells. Cancer Biol Ther. 2006;5:875–83. doi:10.4161/cbt.5.7.2911.